17th World Conference on Earthquake Engineering, 17WCEE
Sendai, Japan - September 13th to 18th 2020

SEISMIC RESPONSE OF STRUCTURES EQUIPPED WITH INERTERS

N. Makris[(1)], G. Moghimi[(2)]

[(1)] *Professor, Southern Methodist Univ, nmakris@mail.smu.edu*
[(2)] *PhD Candidate, Southern Methodist Univ, rmoghimi@mail.smu.edu*

Abstract

This study investigates the seismic response of a two−degrees−of−freedom structure with supplemental rotational inertia at its first story. The proposed response−modification strategy uses an inerter—a mechanical device the resisting force of which is proportional to the relative acceleration between the first story and the ground. This arrangement complements the traditional supplemental damping strategies, which are also examined in this work. The paper develops a time−domain formulation for the response analysis and shows that the seismic protection of structures with supplemental rotational inertia suppresses effectively interstory drifts at the expense of transferring appreciable forces at the support of the inerter. Both a single inerter and a pair of clutching inerters that can only resist the motion of the structure are examined. The paper examines the extent to which a compliant support of the inerter affects the dynamics of the structure and concludes that as the compliance of the support frame increases, a single inerter may lead to a more favorable response. The proposed response−modification strategy is attractive for cases with large relative displacement demands.

Keywords: Inerter; Supplemental Rotational Inertia; Response Modification; Seismic Protection.

1. Introduction

The concept of modifying structural response with supplemental rotational inertia was apparently first introduced in Japan in the late 1990s by Arakaki et al. [1, 2] who proposed a ball−screw assembly to modify the seismic response of structures.

When the lead angle of the screw is appropriate, a ball−screw can be backdriven, producing a force output that is proportional only to the relative acceleration between its end nodes; while storing kinetic energy. Accordingly, a backdriven ball−screw is the precise mechanical analogue of the electrical capacitor in a force−current/velocity−voltage analogy between mechanical and electrical networks. This missing analogy was first recognized by Smith [3] who coined the term "inerter" for any mechanical arrangement where the output force is proportional only to the relative acceleration between its end nodes. For instance, the driving spinning top, in Fig. 1, is a physical realization of the inerter given that the driving force is only proportional to the relative acceleration between nodes 1 and 2. The constant of proportionality of the inerter is coined the "inertance" $= M_R$ [3] and has unit of mass [M]. The unique characteristic of the inerter that it has an appreciable inertial mass as oppose to a marginal gravitational mass. Accordingly, if F_1, u_1 and F_2, u_2 are the forces and displacements at the end nodes of the inerter with inertance , M_R, its constitutive relation is defined as [4, 5]:

$$\begin{Bmatrix} F_1(t) \\ F_2(t) \end{Bmatrix} = \begin{bmatrix} M_R & -M_R \\ -M_R & M_R \end{bmatrix} \begin{Bmatrix} \ddot{u}_1(t) \\ \ddot{u}_2(t) \end{Bmatrix} \tag{1}$$

Smith and his coworkers developed and tested both a rack−and−pinion inerter and a ball−screw inerter [6, 7]. Upon its conceptual development and experimental validation, the inerter was implemented to control the suspension vibrations of racing cars under the name J−damper [8, 9]. In parallel with the aforementioned developments in vehicle mechanics and dynamics and following the pioneering work of Arakaki et al. [1, 2], a growing number of publications have proposed the use of rotational inertia dampers for the wind and seismic protection of civil structures. As an example, Hwang et al. [10] proposed a rotational inertia damper in association with a toggle bracing for vibration control of building structures. Ikago et al. [11] studied the dynamic response of a single−degree−of−freedom (SDOF) structure equipped with a rotational damper that is very similar to the rotational inertia damper initially proposed by Hwang et al. [10]. Their configuration contained an additional flywheel to accentuate the rotational inertia effect of the proposed response modification device. About the same time, Takewaki et al. [12] examined the response of SDOF and multi−degree−of−freedom (MDOF) structures equipped with supplemental rotational inertia offered from a ball−screw−type device that sets in motion a rotating flywheel. More recent studies on the response of MDOF structure equipped with supplemental rotational inertia have been presented by [13−18].

Fig. 1 – A physical realization of the inerter in which the force output is proportional only to the relative acceleration of nodes 1 and 2 and is the mechanical analogue of the capacitor in a force current/velocity-voltage analogy

The aforementioned studies focused invariably on the effectiveness of inrters to reduce structural displacements without looking into the resulting forces and the overall demand in base shear when such response modification devices are used. In a recent paper, Makris and Kampas [19] showed that seismic protection of structures with supplemental rotational inertia is most effective in reducing spectral displacements of long−period SDOF structures at the expense of transferring appreciable forces at the support of the flywheels (chevron frames for buildings or end−abutments for bridges).

Given the effectiveness of supplemental rotational inertia to suppress the seismic displacements of a SDOF system [19], this study investigates the seismic response of the two−degree−of−freedom (2DOF) structure shown in Fig. 2(a). This 2DOF system can be viewed as the idealization of a structure supported on solitary columns, known in modern architecture as a structure on *pilotis*. In this configuration, only the first story (*pilotis*) is engaged to a rotational flywheel system in an effort to investigate to what extent the use of supplemental rotational inertia (use of inerters as a retrofit strategy) can limit large displacements versus the use of large values of supplemental damping. The paper compares the computed response quantities of the 2DOF system in Fig. 2(a) with those when the *pilotis* is retrofitted with large values of supplemental damping [Fig. 2(b)] and with those from the "classical" two−degree−of−freedom system in Fig. 2(c) that has been used to introduce the linear theory of seismic isolation [20, 21].

2. Inertia Forces From the Flywheel Supported on a Stiff Chevron Frame

Fig. 2(a) depicts a 2DOF structure where the mass, m_1, of the first story is engaged to a flywheel with radius R_1 and mass M_{w1} that can rotate about an axis O. We first consider the case of a very stiff chevron frame whose deformation is negligible to the translational displacements, $u_1(t)$ and $u_2(t)$, of the 2DOF structure. Concentric to the flywheel, there is an attached pinion with radius ρ_1 engaged to a linear rack connected to the bottom of the vibrating mass m_1 of the 2DOF. With this arrangement when the mass m_1 undergoes a positive displacement, $u_1(t)$ the flywheel is subjected to a clockwise rotation, $\theta_1(t)$. Given that, there is no slipping between the rack and the pinion

$$\theta_1(t) = \frac{u_1(t)}{\rho_1} \tag{2}$$

With reference to Fig. 2(a) for a positive displacement, $u_1(t)$, to the right, the internal force, $F_I(t)$ at the rack-pinion interface opposes the motion (to the left). Moment equilibrium of the flywheel about point O, gives

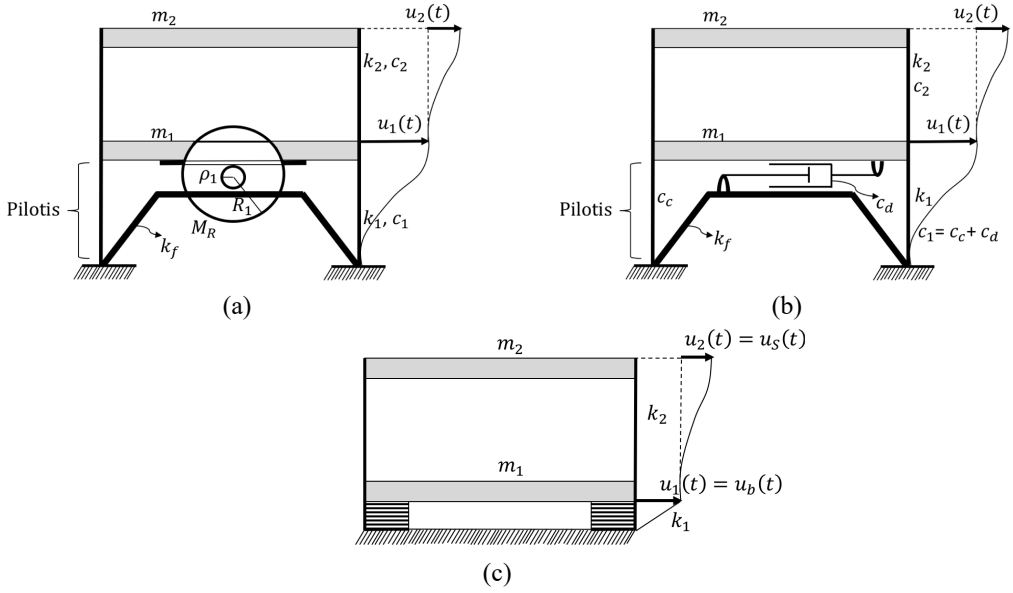

Fig. 2 – (a) 2DOF structure engaged to a rotational flywheel system; (b) 2DOF structure retrofitted with supplemental damper at the first soft story (c) "classical" two-degree-of-freedom seismic isolation system

$$I_{W1}\ddot{\theta}_1(t) = F_I(t)\rho_1 \tag{3}$$

In Eq. (3), $I_{W1} = (1/2)m_{W1}R_1^2$ = moment of inertia of the flywheel about point O. Substituting of Eq. (2) into Eq. (3) gives:

$$F_I(t) = \frac{1}{2}\, m_{W1}\frac{R_1^2}{\rho_1^2}\,\ddot{u}_1(t) = M_R\ddot{u}_1(t) \tag{4}$$

Equation (4) offers the inertial force, $F_I(t)$ at the rack−pinion inerter face−that is the force transferred to the stiff chevron frame. The constant of proportionality, $M_R = (1/2)\, m_{W1}(R^2/\rho_1^2)$ is the inertance of the supplemental rotational inertia system and it has units of mass $[M]$. The inertance, M_R, can be amplified by adding two (or more) flywheels in series, where the first flywheel is a gearwheel [3, 19].

3. Equations of Motion of a 2DOF Structure Supported on a Stiff Chevron Frame

With reference to Fig. 2(a), dynamic equilibrium of the entire structure above the chevron frame gives

$$m_2\left[\ddot{u}_1(t) + \ddot{u}_2(t) + \ddot{u}_g(t)\right] + m_1\left[\ddot{u}_1(t) + \ddot{u}_g(t)\right] = -k_1u_1(t) - c_1\dot{u}_1(t) - F_1(t) \tag{5}$$

where $F_I(t)$ is the internal force from the flywheel given by Eq. (4). Dynamic equilibrium of the second story gives

$$m_2\left[\ddot{u}_1(t) + \ddot{u}_2(t) + \ddot{u}_g(t)\right] = -k_2u_2(t) - c_2\dot{u}_2(t) \tag{6}$$

Following the notation introduced by Kelly [20], the nominal frequencies and nominal damping ratios are

$$\omega_1^2 = \frac{k_1}{m_1+m_2}, \quad \omega_2^2 = \frac{k_2}{m_2} \tag{7}$$

$$2\xi_1\omega_1 = \frac{c_1}{m_1+m_2}, \quad 2\xi_2\omega_2 = \frac{c_2}{m_2} \tag{8}$$

Furthermore, the mass ratio, γ, and the inertance ratio, σ, are defined as:

$$\gamma = \frac{m_2}{m_1+m_2}, \qquad \sigma = \frac{M_R}{m_1+m_2} \tag{9}$$

Equations (5) and (6) can be expressed in matrix form in terms of the parameters defined in Eqs. (7), (8), and (9).

$$\begin{bmatrix}1+\sigma & \gamma\\ 1 & 1\end{bmatrix}\begin{Bmatrix}\ddot{u}_1(t)\\ \ddot{u}_2(t)\end{Bmatrix} + \begin{bmatrix}2\xi_1\omega_1 & 0\\ 0 & 2\xi_2\omega_2\end{bmatrix}\begin{Bmatrix}\dot{u}_1(t)\\ \dot{u}_2(t)\end{Bmatrix} + \begin{bmatrix}\omega_1^2 & 0\\ 0 & \omega_2^2\end{bmatrix}\begin{Bmatrix}u_1(t)\\ u_2(t)\end{Bmatrix} = -\begin{Bmatrix}1\\ 1\end{Bmatrix}\ddot{u}_g(t) \tag{10}$$

When $\sigma = 0$, Eq. (10) is identical to the matrix equation of a two−degree−of−freedom seismic isolated structure [20, 21]. By multiplying Eq. (10) from the left with the inverse of the normalized mass matrix:

$$\begin{bmatrix}1+\sigma & \gamma\\ 1 & 1\end{bmatrix}^{-1} = \begin{bmatrix}\frac{1}{1+\sigma-\gamma} & -\frac{\gamma}{1+\sigma-\gamma}\\ -\frac{1}{1+\sigma-\gamma} & \frac{1+\sigma}{1+\sigma-\gamma}\end{bmatrix} \tag{11}$$

the relative accelerations, $\ddot{u}_1(t)$ and $\ddot{u}_2(t)$, of each story become explicit expressions of the relative displacements, and velocities of the two stories.

$$\ddot{u}_1(t) = -\frac{1-\gamma}{\mu}\,\ddot{u}_g(t) - \frac{2\xi_1\omega_1}{\mu}\,\dot{u}_1(t) + \frac{2\,\gamma\xi_2\omega_2}{\mu}\,\dot{u}_2(t) - \frac{\omega_1^2}{\mu}\,u_1(t) + \frac{\gamma\omega_2^2}{\mu}\,u_2(t) \tag{12}$$

and

$$\ddot{u}_2(t) = -\frac{\sigma}{\mu}\,\ddot{u}_g(t) + \frac{2\xi_1\omega_1}{\mu}\,\dot{u}_1(t) - \frac{2\,(1+\sigma)\xi_2\omega_2}{\mu}\,\dot{u}_2(t) + \frac{\omega_1^2}{\mu}\,u_1(t) - \frac{(1+\sigma)\omega_2^2}{\mu}\,u_2(t) \tag{13}$$

The solution of the system of equations given by Eqs. (12) and (13) is computed numerically via a state−space formulation [22−25] among others. The state vector of the system is

$$\{y(t)\} = < y_1(t), y_2(t), y_3(t), y_4(t) >^T = < u_1(t), \dot{u}_1(t), u_2(t), \dot{u}_2(t) >^T \tag{14}$$

and the time−derivative state vector, $\{\dot{y}(t)\}$ is expressed solely in terms of the state variables appearing in the state vector given by Eq. (14).

$$\{\dot{y}(t)\} = \begin{Bmatrix} \dot{u}_1(t) \\ \ddot{u}_1(t) \\ \dot{u}_2(t) \\ \ddot{u}_2(t) \end{Bmatrix} = \begin{bmatrix} y_2(t) \\ \frac{1}{\mu}\left[-(1-\gamma)\ddot{u}_g(t) - 2\xi_1\omega_1 y_2(t) + 2\gamma\xi_2\omega_2 y_4(t) - \omega_1^2 y_1(t) + \gamma\omega_2^2 y_3(t)\right] \\ y_4(t) \\ \frac{1}{\mu}\left[-\sigma\,\ddot{u}_g(t) + 2\xi_1\omega_1\, y_2(t) - 2(1+\sigma)\xi_2\omega_2\, y_4(t) + \omega_1^2\, y_1(t) - (1+\sigma)\omega_2^2\, y_3(t)\right] \end{bmatrix} \tag{15}$$

where $\mu = 1 + \sigma - \gamma = 1 + (M_R - m_2)/(m_1 + m_2) > 0$.
With reference to Fig. 2, the entire base shear of the structure is

$$V_1(t) = k_1 u_1(t) + c_1\dot{u}_1(t) + M_R\ddot{u}_1(t) = m_2\ddot{u}_2(t) + (m_1 + m_2)\left(\ddot{u}_1(t) + \ddot{u}_g(t)\right) \tag{16}$$

Equation (16) brings forward the role of the inerter in association with the framing action of the first story since the base shear of the structure is proportional to the relative displacement, velocity and acceleration of the first story multiplied with the corresponding lateral stiffness, k_1, damping constant, c_1, and inertance, M_R.

3.1 Two parallel rotational inertia systems

One challenge with the implementation of inerters is that the rotating flywheels should only resist the motion of the structure, without inducing any deformations. This is feasible with the use of a clutch so that the pinion of the first gearwheel that is engaged with the rack is unable to drive the rack and only the motion of the translating rack can drive the pinion−gearwheel [19]. The sequential engagement of the two parallel rotational inertial systems that can only resist the motion is expressed mathematically as [19]

$$\frac{F_I(t)}{m_1} = \sigma\ddot{u}_1(t) \qquad when \quad sgn\left[\frac{\ddot{u}_1(t)}{\dot{u}_1(t)}\right] > 0 \tag{17a}$$

and

$$\frac{F_I(t)}{m_1} = 0 \qquad when \quad sgn\left[\frac{\ddot{u}_1(t)}{\dot{u}_1(t)}\right] \leq 0 \tag{17b}$$

Accordingly, when a pair of clutching inerters is employed, the equations of motion given in Eq. (10) is modified to

$$\begin{bmatrix} 1+\delta\sigma & \gamma \\ 1 & 1 \end{bmatrix}\begin{Bmatrix} \ddot{u}_1(t) \\ \ddot{u}_2(t) \end{Bmatrix} + \begin{bmatrix} 2\xi_1\omega_1 & 0 \\ 0 & 2\xi_2\omega_2 \end{bmatrix}\begin{Bmatrix} \dot{u}_1(t) \\ \dot{u}_2(t) \end{Bmatrix} + \begin{bmatrix} \omega_1^2 & 0 \\ 0 & \omega_2^2 \end{bmatrix}\begin{Bmatrix} u_1(t) \\ u_2(t) \end{Bmatrix} = -\begin{Bmatrix} 1 \\ 1 \end{Bmatrix}\ddot{u}_g(t) \tag{18}$$

in which

$$\delta = \begin{cases} 1, & when \quad sgn\left[\frac{\ddot{u}_1(t)}{\dot{u}_1(t)}\right] > 0 \\ 0, & when \quad sgn\left[\frac{\ddot{u}_1(t)}{\dot{u}_1(t)}\right] \leq 0 \end{cases} \tag{19}$$

Response time histories for an elastic 2DOF oscillator equipped with a single inerter and a pair of clutching inerters have been presented in [26].

Clearly, when a pair of clutching inerters is employed, the flywheels only resist the motion of the structure and do not give back any energy to the structure. During the period when one of the flywheel systems is rotating idly, its rotation needs to decelerate appreciably so that when it is again engaged into motion, it will be capable of resisting the motion through its rotational inertia. This can be achieved by appending an induction generator to the axis of the flywheel, therefore providing an opportunity for energy harvesting.

4. Response Spectra of the 2DOF Structure with a Stiff Chevron Frame

The seismic response of the 2DOF structure equipped with an inerter at the first story as described by Eq. (10) or Eqs. (18) and (19) is compared with the seismic response of the same 2DOF structure where the inerter is replaced with a supplemental viscous damper. In this case the value of the damping coefficient $C_1 = C_c + C_d$, where C_c is the damping originating from the first−story columns and C_d is the damping originating from the supplemental viscous damper. Together with the drift responses $u_1$and u_2 (relative displacements), of interest are the total acceleration of the first story, $\ddot{u}_1 + \ddot{u}_g$, the total acceleration of second story, $\ddot{u}_1 + \ddot{u}_2 + \ddot{u}_g = V_2/m_2$, which is the normalized shear force just above the first story, the total base shear of the structure given by Eq. (16) and the normalized force transferred to the mounting of the flywheel, $F_I(t)/\ (m_1 + m_2)g$, or to the mounting of the supplemental damper, $c_d\dot{u}_1/(m_1 + m_2)g\ = 2\xi_d\omega_1\dot{u}_1/g$.

Fig. 3 shows the recorded acceleration time−history of the Cholame Number 2/360 ground motion recorded during the 2004 Parkfield California earthquake.

The response spectra shown in Figs. 4 are the results of the solution of Eq. (10) for a single inerter (left plots) or Eqs. (18) and (19) when a pair of clutching inerters is used (right plots). When $\sigma = 0$ (thin line), the solution offers the response of the structural systems in Figs. 2(b) and 2(c). For the structural system in Fig. 2(a) values of the normalized inertance $\sigma = 0.5$ and $\sigma = 1.0$ are used. For the structural system in Fig. 2(b) values of $\xi_c = 2\%$ and $\xi_d = 23\%$ are used so that $\xi_1 = \xi_c + \xi_d = 0.02 + 0.23 = 0.25$. In all spectra, the period of the superstructure is $T_2 = 0.2\ sec$, with viscous damping ratio $\xi_2 = 0.02$, and mass ratio, $\gamma = 0.5$.

Fig. 4 presents response spectra for the three configurations of the 2DOF structure in Figs. 2(a), 2(b) and 2(c) when subjected to the Cholame Number 2/360 ground motion recorded during the 2004 Parkfield California earthquake. Across the spectra we indicate two shaded strips. The first strip is for $0.5s \le T_1 \le 1.0s$ and it represents the period range of T_1 for a 2DOF structure with the first story being a *pilotis*. The second shaded strip in the long period range, $T_1 \ge 2.0s$, corresponds to seismic isolated structures.

The first observation in Fig. 4 is that supplemental rotational inertia is most effective in suppressing the displacement of the first story, u_1, in particular for long period structures. When two parallel rotational inertia systems (pair of inerters, right plots) are used, the effectiveness of supplemental rotational inertia [Fig. 2(a)] in suppressing u_1 outperforms the effectiveness of large values of supplemental damping ($\xi_1 = 25\%$) along the entire frequency range. At the same time, in the period range $0.5s \le T_1 \le 1.0s$ the base shear of the entire structure, V_1, is lower when supplemental rotational inertia is used. This situation reverses in the neighborhood of $T_1 = 1.5s$ upon which supplemental damping results in lower base shears. At the same time the forces transferred at the support of the flywheels (chevron frame) are appreciable; however, when a pair of inerters is used these forces are comparable to the case where large values of supplemental damping is used (see bottom plots of Fig. 4).

In view of the results presented in Fig. 4, supplemental rotational inertia ($0.5 \le \sigma \le 1.0$), emerges as an attractive alternative to suppress both displacements and base shears of structures supported on *pilotis*−that is $0.5s \le T_1 \le 1.0s$. Among the three configurations examined, seismic isolation ($T_1 \ge 2.0s$) is most effective in reducing base shears at the expense of producing the largest displacements, u_1. However, isolation systems are designed to accommodate these high displacements above isolators.

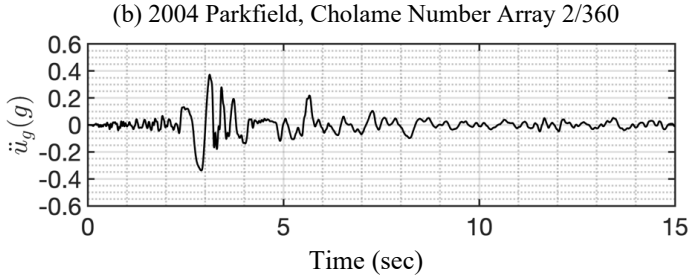

Fig. 3 – Acceleration time history recorded during the 2004 Parkfield, USA earthquake

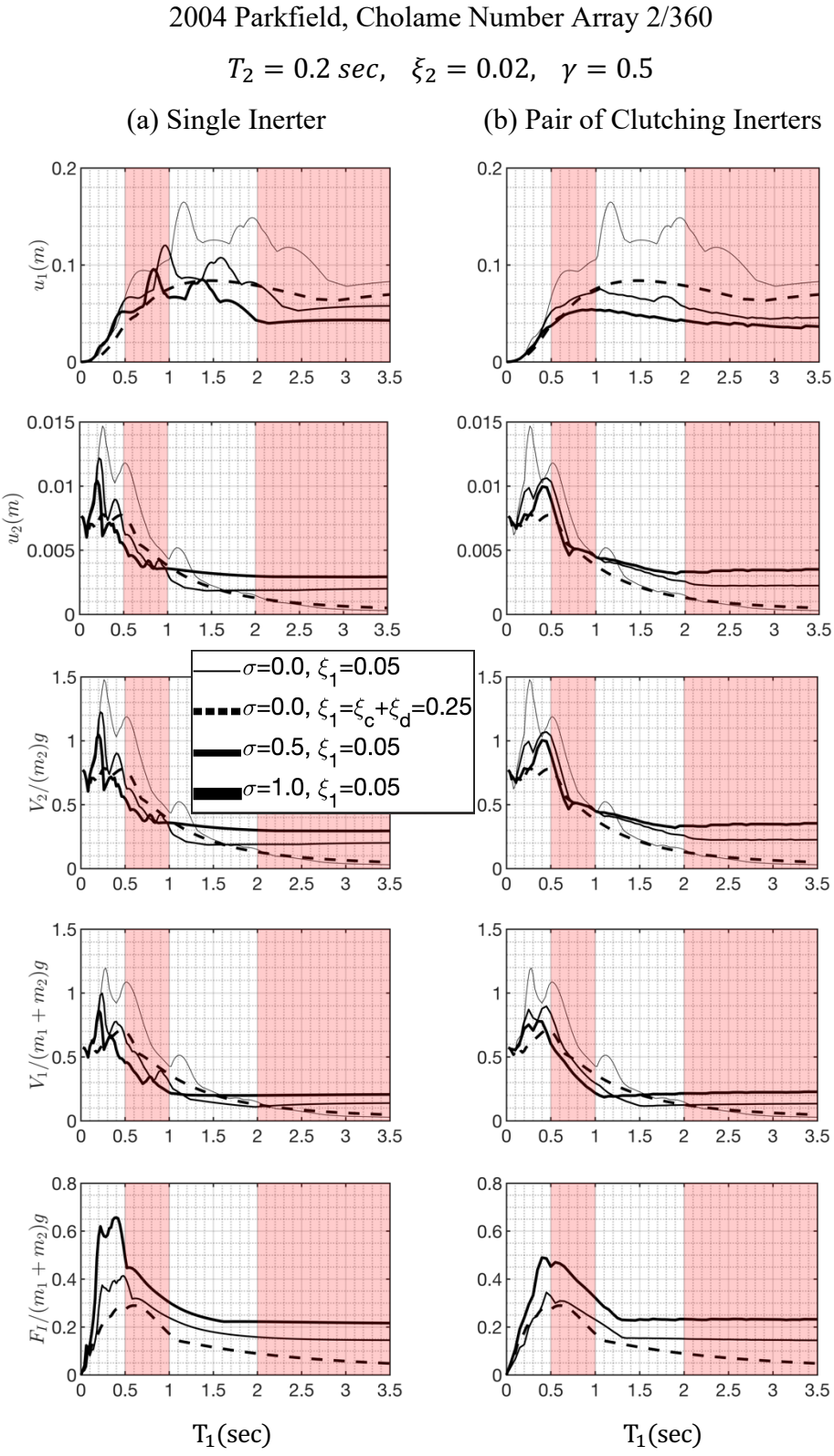

Fig. 4 – Response spectra of a two−degree−of−freedom (2DOF) structure equipped with supplemental rotational inertia (heavy solid lines) or supplemental damping (dashed lines) supported on a stiff frame when excited by the Cholame Number 2/360 ground motion recorded during the 2004 Parkfield, USA earthquake

5. Equations of Motion of a 2DOF Structure with a Compliant Chevron Frame with Finite Stiffness and Damping

Now the case where the chevron frame that supports the rotational inertia system shown in Fig. 2(a) has a finite stiffness, k_f, and damping constant, c_f, is considered. Because of its compliance, under the force transferred by the mounting of the flywheel, the chevron frame deforms and this deformation, influences the resisting force, $F_I(t)$, from the flywheel. Accordingly, $F_I(t)$, is no longer expressed with Eq. (4)−that is for a rigid chevron frame, but from [19, 5].

$$F_I(t) + \lambda \frac{dF_I(t)}{dt} + \frac{1}{\omega_R^2} \frac{d^2F_I(t)}{dt^2} = M_R \left(\frac{d^2u_1(t)}{dt^2} + \lambda \frac{d^3u_1(t)}{dt^3} \right) \tag{20}$$

In which the relaxation time, $\lambda = c_f/k_f$ and the rotational frequency $\omega_R = \sqrt{k_f/M_R}$ [27, 5]. Equation (20) is the constitutive law of a spring−dashpot parallel connection (k_f, c_f) that is connected in series with an inerter (M_R). This mechanical network is also known as the tuned inerter damper (TID) [16], and was coined recently as the inertoviscoelastic fluid A [5]. The term "fluid" expresses that the network undergoes infinite displacement under a static loading.

The equations of motion of the 2DOF structure in Fig. 2(a) are given by Eqs. (5) and (6); however, now for the case of a chevron frame with finite stiffness, k_f, and damping, c_f, the force from the flywheel, $F_I(t)$ appearing in Eq. (4) is described by Eq. (20).

By using the frequencies, damping, mass and inertance ratios defined by Eqs. (7)−(9), the equations of motion of the 2DOF structure in Fig. 2(a) with a compliant chevron frame with finite stiffness, k_f, and damping, $c_f = \lambda k_f$ can be expressed in matrix form.

$$\begin{bmatrix} 1 & \gamma \\ 1 & 1 \end{bmatrix} \begin{Bmatrix} \ddot{u}_1(t) \\ \ddot{u}_2(t) \end{Bmatrix} + \begin{bmatrix} 2\xi_1\omega_1 & 0 \\ 0 & 2\xi_2\omega_2 \end{bmatrix} \begin{Bmatrix} \dot{u}_1(t) \\ \dot{u}_2(t) \end{Bmatrix} + \begin{bmatrix} \omega_1^2 & 0 \\ 0 & \omega_2^2 \end{bmatrix} \begin{Bmatrix} u_1(t) \\ u_2(t) \end{Bmatrix} = -\begin{bmatrix} 1 & 1 \\ 0 & 1 \end{bmatrix} \begin{Bmatrix} \frac{F_I(t)}{m_1+m_2} \\ \ddot{u}_g(t) \end{Bmatrix} \tag{21}$$

in which $F_I(t)$ is solution of Eq. (20).

By multiplying Eq. (21) from the left with the inverse of the normalized mass matrix [26] the relative accelerations, $\ddot{u}_1(t)$, and $\ddot{u}_2(t)$ are expressed as

$$\ddot{u}_1(t) = -\frac{1}{1-\gamma} f_I(t) - \ddot{u}_g(t) - \frac{2\xi_1\omega_1}{1-\gamma} \dot{u}_1(t) + \frac{2\gamma\xi_2\omega_2}{1-\gamma} \dot{u}_2(t) - \frac{\omega_1^2}{1-\gamma} u_1(t) + \frac{\gamma\omega_2^2}{1-\gamma} u_2(t) \tag{22}$$

$$\ddot{u}_2(t) = \frac{1}{1-\gamma} f_I(t) + \frac{2\xi_1\omega_1}{1-\gamma} \dot{u}_1(t) - \frac{2\xi_2\omega_2}{1-\gamma} \dot{u}_2(t) + \frac{\omega_1^2}{1-\gamma} u_1(t) - \frac{\omega_2^2}{1-\gamma} u_2(t) \tag{23}$$

where $f_I(t) = F_I(t)/(m_1 + m_2)$ has units of acceleration.
In this case, the state vector of the system is

$$\{y(t)\} = < y_1(t), y_2(t), y_3(t), y_4(t), y_5(t), y_6(t) >^T = < u_1(t), \dot{u}_1(t), u_2(t), \dot{u}_2(t), f_I(t), \dot{f}_I(t) >^T \tag{24}$$

From Eq. (20) it is evident that the time−derivative of $y_6(t)$, that is $\dot{y}_6(t) = \ddot{f}_1(t)$, involves the third derivative of $u_1(t)$ which is given by

$$\dddot{u}_1(t) = -\frac{1}{1-\gamma} \dot{f}_I(t) - \dddot{u}_g(t) - \frac{2\xi_1\omega_1}{1-\gamma} \ddot{u}_1(t) + \frac{2\gamma\xi_2\omega_2}{1-\gamma} \ddot{u}_2(t) - \frac{\omega_1^2}{1-\gamma} \dot{u}_1(t) + \frac{\gamma\omega_2^2}{1-\gamma} \dot{u}_2(t) \tag{25}$$

In terms of the state variables given by Eq. (24), Eq. (25) assumes the form

$$\begin{aligned} \dddot{u}_1(t) = & -\left(\frac{1}{1-\gamma} y_6(t) + \dddot{u}_g(t) \right) - \frac{2\xi_1\omega_1}{1-\gamma} \left(-\frac{1}{1-\gamma} y_5(t) - \ddot{u}_g(t) - \frac{2\xi_1\omega_1}{1-\gamma} y_2(t) + \frac{2\gamma\xi_2\omega_2}{1-\gamma} y_4(t) - \frac{\omega_1^2}{1-\gamma} y_1(t) + \frac{\gamma\omega_2^2}{1-\gamma} y_3(t) \right) \\ & + \frac{2\gamma\xi_2\omega_2}{1-\gamma} \left(\frac{1}{1-\gamma} y_5(t) + \frac{2\xi_1\omega_1}{1-\gamma} y_2(t) - \frac{2\xi_2\omega_2}{1-\gamma} y_4(t) + \frac{\omega_1^2}{1-\gamma} y_1(t) - \frac{\omega_2^2}{1-\gamma} y_3(t) \right) - \frac{\omega_1^2}{1-\gamma} y_2(t) + \frac{\gamma\omega_2^2}{1-\gamma} y_4(t) \end{aligned} \tag{26}$$

The solution of the system of differential equations given by Eqs. (20), (22) and (23) is computed by integrating the time−derivative of the state vector given by Eq. (24)

$$\{\dot{\boldsymbol{y}}(\boldsymbol{t})\} = \begin{Bmatrix} \dot{u}_1(t) \\ \ddot{u}_1(t) \\ \dot{u}_2(t) \\ \ddot{u}_2(t) \\ \dot{f}_I(t) \\ \ddot{f}_I(t) \end{Bmatrix} = \begin{Bmatrix} y_2(t) \\ -\frac{1}{1-\gamma} y_5(t) - \ddot{u}_g(t) - \frac{2\xi_1\omega_1}{1-\gamma} y_2(t) + \frac{2\gamma\xi_2\omega_2}{1-\gamma} y_4(t) - \frac{\omega_1^2}{1-\gamma} y_1(t) + \frac{\gamma\omega_2^2}{1-\gamma} y_3(t) \\ y_4(t) \\ \frac{1}{1-\gamma} y_5(t) + \frac{2\xi_1\omega_1}{1-\gamma} y_2(t) - \frac{2\xi_2\omega_2}{1-\gamma} y_4(t) + \frac{\omega_1^2}{1-\gamma} y_1(t) - \frac{\omega_2^2}{1-\gamma} y_3(t) \\ y_6(t) \\ \omega_R^2\sigma\big(\ddot{u}_1(t) + \lambda\ddot{u}_1(t)\big) - \omega_R^2 y_5(t) - \omega_R^2\lambda\, y_6(t) \end{Bmatrix} \tag{27}$$

In the last row of Eq. (27), the acceleration of the first story, $\ddot{u}_1(t)$, is given by the second row of Eq. (27) and the derivative of the acceleration, $\dddot{u}_1(t)$, is given by Eq. (26). The numerical integration of Eq. (27) is performed with standard ordinary differential equation (ODE) solvers available in MATLAB.

When the two parallel rotational inertia system (pair of inerters) is employed that can only resist the motion of the structure without inducing any deformation (the pinion of the gearwheel that is engaged in the rack of the first story is unable to drive the rack and only the motion of the translating rack can drive the pinion), the normalized force, $f_I(t) = F_I(t)/(m_1 + m_2)$ appearing in Eqs. (22) and (23) is given by Eq. (20) when $sgn\,[\ddot{u}_1(t)/\dot{u}_1(t)] \geq 0$ and by

$$f_I(t) = \frac{F_I(t)}{m_1+m_2} = 0 \qquad when \;\; sgn\left[\frac{\ddot{u}_1(t)}{\dot{u}_1(t)}\right] < 0 \tag{28}$$

In the case when $f_I(t) = 0$, the equations of motion of our 2DOF structure become piecewise linear and only a time − domain solution is feasible. The state vector of the system is given by Eq. (27) when $sgn\,[\ddot{u}_1(t)/\dot{u}_1(t)] > 0$ and by

$$\{\dot{y}(t)\} = \begin{Bmatrix} \dot{u}_1(t) \\ \ddot{u}_1(t) \\ \dot{u}_2(t) \\ \ddot{u}_2(t) \end{Bmatrix} = \begin{bmatrix} y_2(t) \\ -\ddot{u}_g(t) - \frac{2\xi_1\omega_1}{1-\gamma} y_2(t) + \frac{2\gamma\xi_2\omega_2}{1-\gamma} y_4(t) - \frac{\omega_1^2}{1-\gamma} y_1(t) + \frac{\gamma\omega_2^2}{1-\gamma} y_3(t) \\ y_4(t) \\ -\ddot{u}_g(t) - \frac{2\xi_1\omega_1}{1-\gamma} y_2(t) + \frac{2\gamma\xi_2\omega_2}{1-\gamma} y_4(t) - \frac{\omega_1^2}{1-\gamma} y_1(t) + \frac{\gamma\omega_2^2}{1-\gamma} y_3(t) \end{bmatrix} \tag{29}$$

when $sgn\,[\ddot{u}_1(t)/\dot{u}_1(t)] < 0$.

6. Response Spectra of the 2DOF Structure with a Compliant Chevron Frame with Finite Stiffness and Damping

The response spectrum shown in Fig. 5 are the results of the solution of Eq. (27) (single inerter with a time−domain formulation) and Eqs. (27) and (29) when a pair of clutching inerters is used. Again, when $\sigma = 0$, the solution offers the response of the structural systems in Figs. 2(b) and 2(c). For the structural system in Fig. 2(a), values of the normalized inertance, $\sigma = 0.5$ and $\sigma = 1.0$ are used. The compliance of the chevron frame is expressed with the relaxation time, $\lambda = c_f/k_f = 0.05$, while the stiffness of the chevron frame compared to the supplemental inertance M_R, is expressed with the dimensionless product $\lambda\omega_R = 0.5$. For the structural system in Fig. 2(b), values of $\xi_c = 2\%$ and $\xi_d = 23\%$ are used so that $\xi_1 = \xi_c + \xi_d = 0.25$. When supplemental damping c_d, is used, the compliance of the chevron frame is $\lambda_1 = \big(c_d + c_f\big)/k_f = 0.5$ (details in [26]). In all spectra, the period of the superstructure is $T_2 = 0.2$ with viscous damping ratio $\xi_2 = 0.02$ and mass ratio $\gamma = 0.5$. Fig. 5 presents response spectra for the three configuration of the 2DOF structure in Fig. 2 when the chevron frame has finite stiffness k_f and damping c_f and is subjected to the Cholame Number 2/360 ground motion recorded during the 2004 Parkfield, USA earthquake. Across the spectra we indicate the same two shaded strips as explained when discussing the spectra shown in Fig. 4.

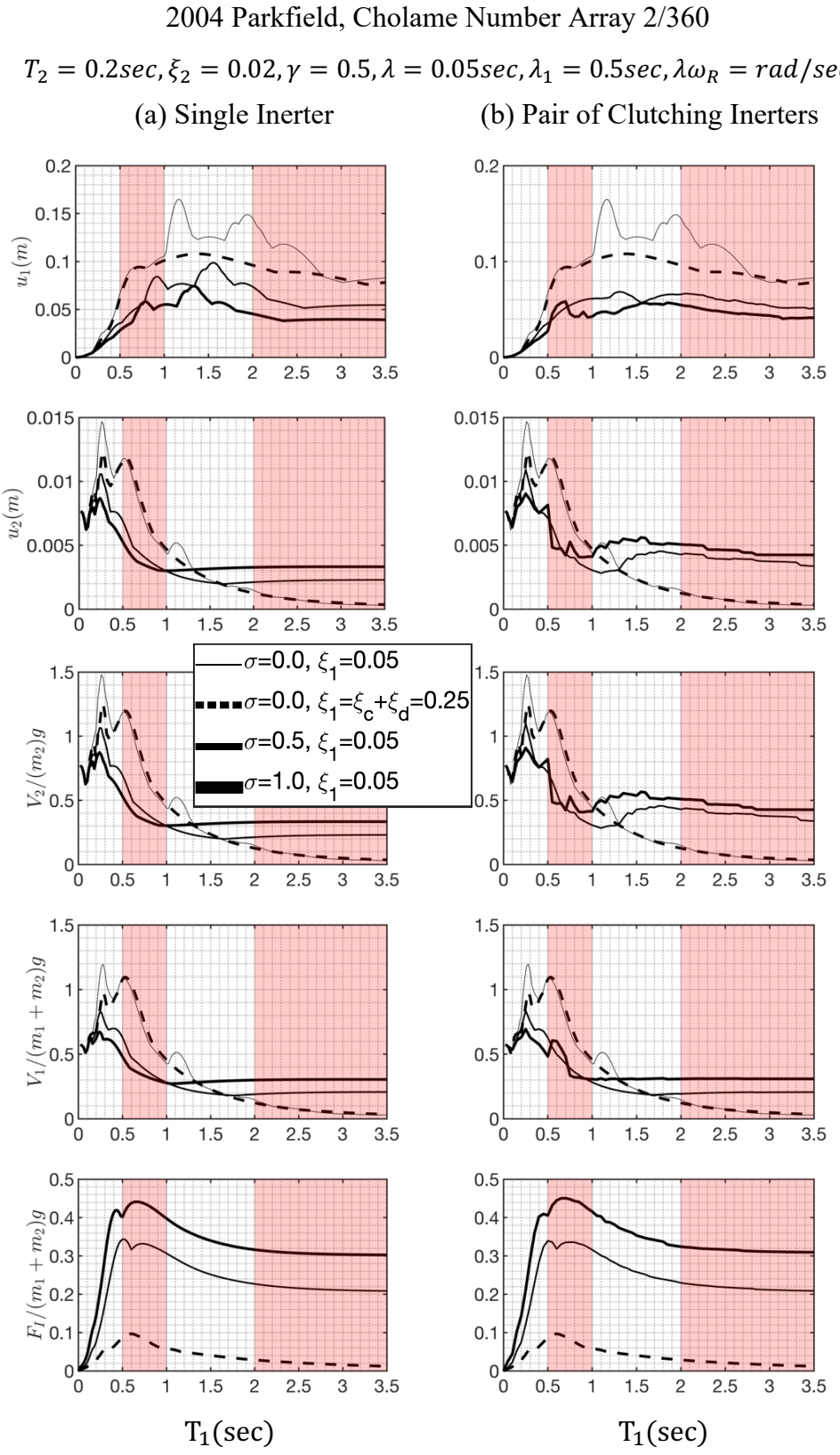

Fig. 5 – Response spectra of a two−degree−of−freedom (2DOF) structure equipped with supplemental rotational inertia (heavy solid lines) or supplemental damping (dashed lines) supported on a compliant frame when excited by the Cholame Number 2/360 ground motion recorded during the 2004 Parkfield, USA earthquake

The first observation in Fig. 5 is that even when a compliant chevron frame is used, supplemental rotational inertia remains on effective strategy in suppressing displacements of the first story, u_1, along the entire frequency range. Interestingly, Fig. 5 reveals, that the compliance of the chevron frame reduces the effectiveness of the pair of clutching inerters (right plots) when compared to the case of a single inerter (left plots) which produces the most favorable response other than increasing the forces transferred to the chevron frame (bottom plots). In summary, the results presented in Fig. 5 in association with the results presented in Figs. 4 (for a stiff chevron frame) reveal that supplemental rotational inertia is an effective response modification strategy for controlling the response of a structure with a soft first−story at the expense of transferring appreciable forces at the support of the inerter. Accordingly, assuming that the chevron frame is properly designed, supplemental rotational inertia is a competitive alternative to the use of supplemental damping, in particular for cases with large relative displacement demands.

7. Conclusions

This paper investigates the potential advantages of using supplemental rotational inertia for the seismic protection of moment−resisting frames. The paper examines the response of a 2DOF structure where the first story employs a rack−pinion−flywheel system whose resisting force is proportional to the relative acceleration between the vibrating mass and the support of the flywheels. Both cases of a stiff and a compliant support of the inerter is examined and the corresponding equations of motion have been derived. The paper shows that the supplemental rotational inertia controls effectively the displacements of the first story along a wide range of the response spectrum. Furthermore, the proposed seismic protection strategy can accommodate large relative displacements without suffering from the issue of viscous heating [27−29] and potential leaking that challenges the implementation of fluid dampers under prolonged cyclic loading.

The paper examines the dynamic response of the 2DOF structure when two parallel rotational inertia systems are installed so that they can only resist the motion of the structure without inducing any deformation. This can be achieved with a pair of inerters and the use of a simple clutch [19]. When the chevron frame that supports the rotational inertia system is stiff, the use of two parallel rotational inertia systems offers improved results for the response of the 2DOF structure. However, as the compliance of the chevron frame that supports the inerters increases, the use of a single rotational inertia system offers more favorable response other than increasing the forces transferred to the chevron frame.

8. References

[1] Arakaki T, Kuroda H, Arima F, Inoue Y, Baba K (1999a): Development of seismic devices applied to ball screw: part 1 basic performance test of RD−series (in Japanese). *AIJ Journal of Technology and Design*, **5** (8), 239−244.

[2] Arakaki T, Kuroda H, Arima F, Inoue Y, Baba K (1999b): Development of seismic devices applied to ball screw: part 2 performance test and evaluation of RD-series (in Japanese). *AIJ Journal of Technology and Design*, **5** (9), 265−270.

[3] Smith M (2002): Synthesis of mechanical networks: the inerter. *IEEE Transactions on Automatic Control*. **47**(10), 1648−1662.

[4] Saitoh M (2007): Simple model of frequency−dependent impedance functions in soil−structure interaction using frequency−independent elements. *Engineering Mechanics*, *ASCE,* **133**(1),11101−1114.

[5] Makris N (2018): Time−response functions of mechanical networks with inerters and causality. *Meccanica*, **53**(1), 2237–2255.

[6] Papageorgiou C, Smith M (2005): Laboratory experimental testing of inerters. *Proceedings of the 44th IEEE Conference on Decision and Control*. Seville, Spain.

[7] Papageorgiou C, Houghton N, Smith M (2008): Experimental testing and analysis of inerter devices. *Dynamic Systems Measurement and Control*, **131**(1), 011001-1− 011001-11.

[8] Chen M, Papageorgiou C, Scheibe F, Wang F, Smith M (2009): The missing mechanical circuit. *IEEE Circuits and Systems Magazine,* **9**(1),10−26.

[9] Kuznetsov A, Mammadov M, Sultan I, Hajilarov E (2011): Optimization of improved suspension system with inerter device of the quarter−car model in vibration analysis. *Archive of Applied Mechanics*, **81**(10), 1427−1437.

[10] Hwang J, Kim J, Kim Y (2007): Rotational inertia dampers with toggle bracing for vibration control of a building structure. *Engineering Structures*, **29**(6), 1201−1208.

[11] Ikago K, Saito K, Inoue N (2012): Seismic control of single degree-of-freedom structure using tuned viscous mass damper. *Earthquake Engineering and Structural Dynamics*, **41**(3), 453−474.

[12] Takewaki I, Murakami S, Yoshitomi S, Tsuji M (2012): Fundamental mechanism of earthquake response reduction in building structures with inertial dampers. *Structural Control and Health Monitoring*, **19**(6), 590−608.

[13] Ishii M, Kazama H, Miyazaki K, Murakami K (2014): Application of Tuned Viscous Mass Damper to Super−High-Rise Buildings. *Sixth World Conference of the International Association for Structural Control and Monitoring*. Barcelona, Spain.

[14] Marian L, Giaralis A (2014): Optimal design of a novel tuned mass damper−inerter (TMDI) passive vibration control configuration for stochastically support−excited structural systems. *Probabilistic Engineering Mechanics*, **38**(1), 156–164.

[15] Lazar I, Neild S, Wagg D (2014): Using an inerter−based device for structural vibration suppression. *Earthquake Engineering and Structural Dynamics.* **43**(8):1129−1147.

[16] Chen M, Hu Y, Huang L, Chen G (2014): Influence of inerter on natural frequencies of vibration systems. *Sound and Vibration*, **333**(7), 1874–1887.

[17] Giaralis A, Taflanidis A. (2017): Optimal tuned−mass−damper−inerter (TMDI) design for seismically excited MDOF structures with model uncertainties based on reliability criteria. *Structural Control and Health Monitoring*, **25**(2), e2082.

[18] De Domenico D, Ricciardi G (2018): Optimal design and seismic performance of tuned mass damper inerter (TMDI) for structures with nonlinear base isolation systems. *Earthquake Engineering and Structural Dynamics*. **47**(12), 2539−2560.

[19] Makris N, Kampas G (2016): Seismic protection of structures with supplemental rotational inertia. *Engineering Mechanics*. **142**(11), 04016089.

[20] Kelly J (1997): *Earthquake−Resistant Design with Rubber*, Springer, London.

[21] Kelly J, Konstantinidis D (2011): *Mechanics of Rubber Bearings for Seismic and Vibration Isolation.* Wiley, Chichester, U.K.

[22] Konstantinidis D, Makris N (2005): Seismic response analysis of multidrum classical columns. *Earthquake Engineering and Structural Dynamics.* **34**(10), 1243–1270.

[23] Pitilakis D, Makris N (2010): Dimensional Analysis of Inelastic Systems with Soil−Structures Interaction, *Bulletin of Earthquake Engineering*, **8**(6), 1497–1514.

[24] Vassiliou, M. F., and Makris, N. (2012). "Analysis of the rocking response of rigid blocks standing free on a seismically isolated base". *Earthquake Engineering and Structural Dynamics*, **41**(2), 177–196.

[25] Aghagholizadeh M, Makris N (2017): Seismic response of a yielding structure coupled with a rocking wall. *Structural Engineering, ASCE*, **144** (2), 04017196.

[26] Makris N, Moghimi G (2019): Displacements and forces in structures with inerters when subjected to earthquakes. *Structural Engineering, ASCE,* **145**(2):04018260.

[27] Makris N. (1998): Viscous heating of fluid dampers I: small amplitude motions, *Engineering Mechanics,(ASCE)*, **124**(11), 1210−1216.

[28] Makris N, Roussos Y, Whittaker S, Kelly J (1998): Viscous heating of fluid dampers ii: large-amplitude motions. *Engineering Mechanics,(ASCE)*, **124**(11), 1210–1216.

[29] Black C, Makris N (2007): Viscous heating of fluid dampers under small and large amplitude motions: experimental studies and parametric modeling. *Engineering Mechanics,(ASCE),* **133**(5), 1210–1216.

